

OPEN ACCESS

An asymmetrical λ -foot of condensing steam flow in the IMP PAN nozzle

To cite this article: S Kornet and J Badur 2014 *J. Phys.: Conf. Ser.* **530** 012018

View the [article online](#) for updates and enhancements.

You may also like

- [Silver Nanoparticle-Decorated Carbon Fiber Microelectrode for Imidacloprid Insecticide Analysis](#)
Keerakit Kaewket and Kamonwad Ngamchuea
- [Mathematical calibration procedure of a capacitive sensor-based indexed metrology platform](#)
A Brau-Avila, J Santolaria, R Acero et al.
- [Mechanism for the Morphological Change from Trenching to Pitting around Intermetallic Particles in AA1050 Aluminum](#)
Hiroshi Kakinuma, Izumi Muto, Yoshiyuki Oya et al.



ECS
The
Electrochemical
Society
Advancing solid state &
electrochemical science & technology

DISCOVER
how sustainability
intersects with
electrochemistry & solid
state science research

An asymmetrical λ -foot of condensing steam flow in the IMP PAN nozzle

S Kornet^{1,2*} and J Badur¹

¹Energy Conversion Department, Institute of Fluid-Flow Machinery PAS-ci, Gdańsk, Poland

²Conjoint Doctoral School at the Faculty of Mechanical Engineering, Gdansk University of Technology, Gdańsk, Poland

E-mail: sebastian.kornet@imp.gda.pl, jb@imp.gda.pl

Abstract. In the present paper we have focused on the precise prediction of the spontaneous condensation phenomena in wet steam flow. Novelty of our approach lies on modelling both the moment of initiation of a phase transition, as well as the moment of its reverse progress - called here re-vaporization of the condensate phase. The practical issue is to elaborate of a model of spontaneous condensation/vaporization of water steam flow under low-pressure conditions by using methodology of non-equilibrium thermodynamics [2]. The basic tests including comparison with an experimental data have been performed using the IMP PAN nozzle with the de Laval geometry [1]. Having observed the finishing of a foggy flow within the shock wave, according to Puzyrewski's postulate [1], we would like to analyse the topography of the shock wave pattern in the IMP PAN symmetric nozzle. This phenomenon, independently from a type of compressible fluid, has been observed to be the result of interaction between a normal shock wave and the boundary layer – it has been known as a λ -foot structure [3]. The asymmetry of the shock structure is measured by optical system and visible since the foggy flow can be easily observed. Our paper is a trial towards to an explanation of this problem.

1. Introduction

The first time the de Laval nozzle has been used in steam turbines in 1888. Nowadays nozzles are commonly used to acceleration different fluids in various technical devices.

In the low-pressure part of steam turbine, the state path usually crosses the saturation line in penultimate stages. At least last two stages of this part of turbines operate in two-phase region. The liquid phase in this region is mainly created in the process of homogeneous and heterogenous condensation. Several observations confirm however, that condensation often occurs earlier than it is predicted by theory i.e. before the Wilson line. It is because the nucleation can start at some soluble and insoluble impurities, particle of dust, chemical compounds or corrosion products. Droplets of condensed phase can move with velocity different than gas phase velocity and can seriously damage blades. Erosion of rotor blade leading edge is mainly due to droplets that form behind the trailing edge of guide vanes. The flow in the low-pressure part of steam turbine is complicated and still requires thorough experimental and numerical analysis [5, 6].

Shock wave is the result of interaction between a normal shock wave and the boundary layer, which produces a λ -foot structure. It is well-known and experimentally confirmed that for low Mach



numbers the λ -feet are of the same size at both nozzle walls. However, at higher velocities ($Ma > 1.4$) the λ -feet generated on the upper and lower walls of a symmetric nozzle become different in size. Flow separation inside propulsive nozzles generates unsteady and asymmetrical shock structures and induce fluctuating side loads which can damage the structure. It has also been observed that the tendency towards asymmetry depends on the nozzle divergence angle [3, 7, 8, 9]. The most of the experimental data used for validation of the numerical models are relatively old, and do not include a precise investigation of the shock wave behaviour in the wet steam regime.

The present work is concerned with investigation into coupled phenomena occurring in the supersonic section of the de Laval nozzle, characterized by the presence of shock the flow of condensing steam.

2. Conditions of experiment

The experiment was carried out in a symmetric nozzle of rectangular cross-section. The nozzle dimensions and variation of cross section area along the nozzle axis are shown in figure 1. The nozzle inlet conditions were varied within a rather narrow range by throttling or by injecting water into superheated steam. The exhaust pressure was varied by flow throttling in the pipeline leading steam out to the condenser. Thus it was possible to change the location of the shock wave within the supersonic section of the nozzle. The pressure measurements were made on both side walls of the channel. Initial parameters were close to the saturation line, in order to obtain a condensation [4].

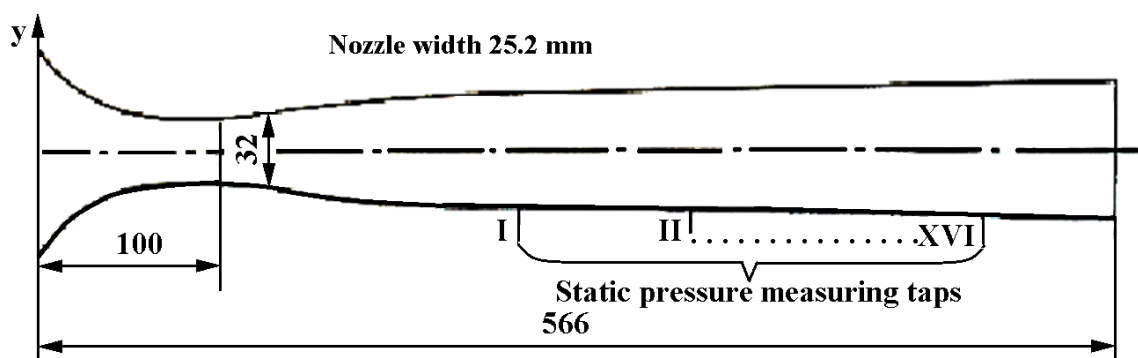


Figure 1. The shape and dimensions of the IMP PAN nozzle [4].

3. Conditions of numerical analysis

Modelling conditions have been taken from description of experiment [4] that was originally conducted at Institute of Fluid-Flow Machinery site. Inlet pressure was $p_{inlet} = 2.26$ bar, inlet temperature $T_{inlet} = 502.15$ K. Pressure at the point of intersection of the isentropic expansion line and saturation line was $p_{sat} = 0.55$ bar. These input conditions correspond to the V-th set of experimental conditions [4]. Nozzle geometry, was prepared within preprocessing utility Gambit version 2.4.6. The mesh was generated very precisely to eliminate any incidental asymmetry. Mesh for full geometry of the nozzle (figure 2) has consisted of 380000 hexahedral finite volumes.

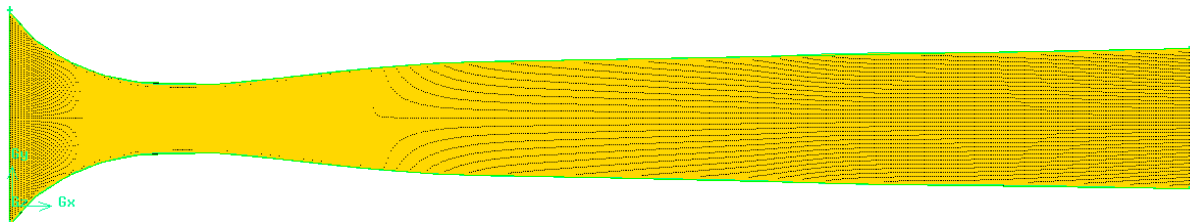


Figure 2. FVM discretization of the de Laval nozzle.

4. Governing equations of CFD and assumptions for a employed model.

Wet steam governing equations are based on the following balance of liquid-vapour mixture:

- balance of mass – ρ :

$$\partial_t(\rho) + \text{div}(\rho \mathbf{v}) = 0 \quad (1)$$

- balance of momentum – $\rho \mathbf{v}$:

$$\partial_t(\rho \mathbf{v}) + \text{div}(\rho \mathbf{v} \otimes \mathbf{v} + p \mathbf{I}) = \text{div}(\boldsymbol{\tau}^c) + \rho \mathbf{b} \quad (2)$$

- balance of energy – e :

$$\partial_t(\rho e) + \text{div}(\rho e \mathbf{v} + p \mathbf{v}) = \text{div}(\boldsymbol{\tau}^c \mathbf{v} + \mathbf{q}^c) + \rho \mathbf{b} \cdot \mathbf{v} \quad (3)$$

- turbulence energy evolution – k :

$$\partial_t(\rho k) + \text{div}(\rho k \mathbf{v}) = \text{div}(\mathbf{J}_k) + \rho S_k \quad (4)$$

- turbulence dissipation evolution – ε :

$$\partial_t(\rho \varepsilon) + \text{div}(\rho \varepsilon \mathbf{v}) = \text{div}(\mathbf{J}_\varepsilon) + \rho S_\varepsilon \quad (5)$$

- evolution of wetness fraction – x :

$$\partial_t(\rho x) + \text{div}(\rho x \mathbf{v}) = \text{div}(\mathbf{J}_x) + \rho S_x \quad (6)$$

- evolution of number of droplets – a :

$$\partial_t(\rho a) + \text{div}(\rho a \mathbf{v}) = \text{div}(\mathbf{J}_a) + \rho S_a \quad (7)$$

An additional balance equations for k , ε , x and a are related to the evolution of turbulence in the condensing flow, or the condensation evolution under turbulent flow condition. Both are fully non-equilibrium phenomena, that should be combined by the sources S , and thermodynamical forces which constitute fluxes \mathbf{J} . The above set of nine equations is to be integrated within every finite volume [5, 10,11,]. The following assumptions are made in this model:

- the velocity slip between the droplets and gaseous-phase is negligible,
- the interactions between droplets are neglected,
- the mass fraction of the condensed phase is small: $\beta < 0.2$ (wetness factor),

- since droplet sizes are typically very small (from approximately 0.1 microns to approximately 100 microns), it is assumed that the volume of the condensed liquid phase is negligible [10, 11].

5. Results and discussion

For a given de Laval nozzle geometry authors have conducted calculations for wet steam model. Our numerical investigation (figure 3a) have shown that for low Mach numbers the feet are of the same size. However, at higher velocities ($Ma > 1.4$), the λ -feet generated on the upper and lower walls of a symmetric nozzle become different in size (figure 3b). λ -feet is result of interaction between a normal shock wave and the boundary layer.

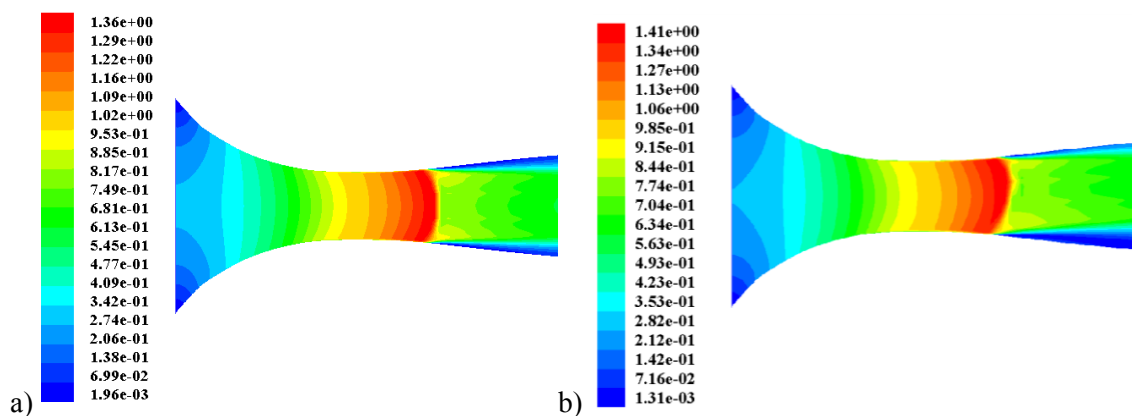


Figure 3. Shock wave: a) symmetric pattern for low Mach number, b) asymmetric pattern for Mach number higher than 1.4.

The shock/boundary layer interaction produces two separated flows: 1 - with reattachment downstream for upper wall (this is a restricted shock separation) and 2 - without reattachment downstream for lower wall (this is a free shock separation). The interaction between the two oblique shocks (C1 and C3 in figure 4a) forms a Mach disc (MD). The λ -shock structures C1 – C2 and C3 – C4 are jointed to Mach disc by two triple points T1 and T2. Above the critical pressure ratio $p_{inlet}(p_{outlet})^{-1}$ shock wave becomes symmetrical with respect to the nozzle axis again, what we can see in figure 4b.

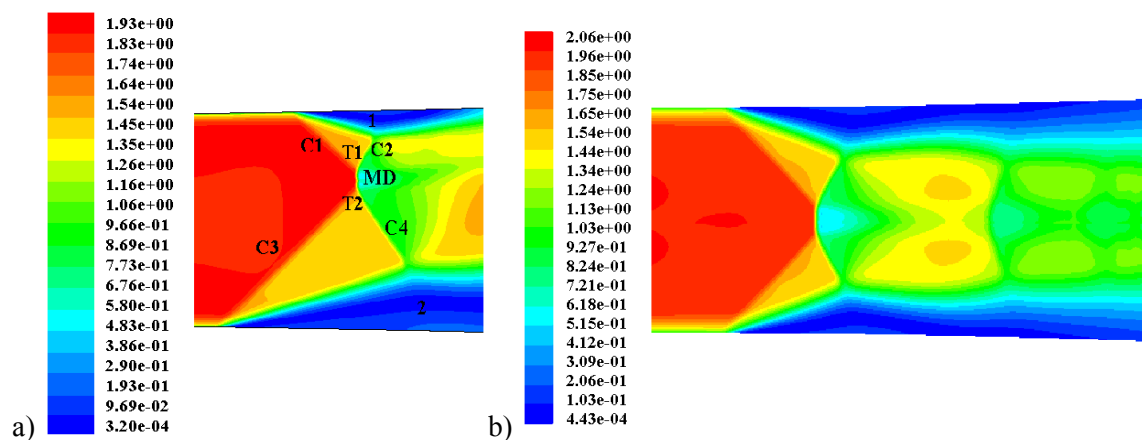


Figure 4. Shock wave: a) asymmetrical shock pattern for $Ma > 1.4$, b) symmetrical shock pattern above the critical pressure ratio.

Visual observations (in the experiment) were carried out either with direct lighting, or marking use of the Töpler optical system to improve the possibility of indentifying shock wave. In the figure 5a we can see shock wave photo taken using this optical system and in figure 5b we can see the same shape and localization of shock for CFD simulation for the same flow conditions.

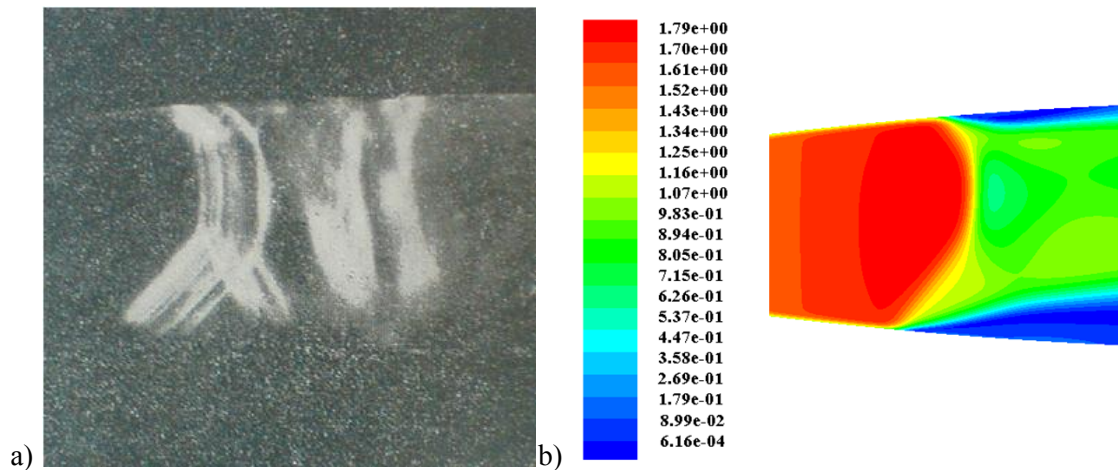


Figure 5. The same localization and shape of shock in the nozzle a) experiment, b) CFD simulation.

Figure 6 shows a comparison of the results of the experiment with nine-equation non-equilibrium model of wet steam for the V-th set of experimental conditions. This model of condensation provides a good agreement with experiment. Figure 7 presents expansion in the „i-s” diagrams for chosen flow conditions obtained by numerical analysis. In the figure 8 we can see this expansion in wet steam region. Phenomena such as: shock, condensation and evaporation cause that the expansion in wet steam region is very complicated.

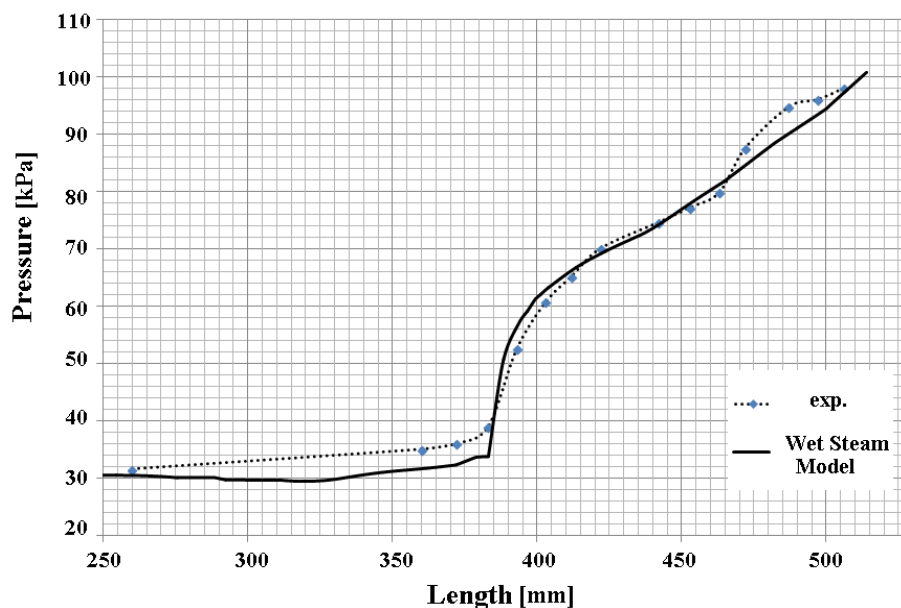


Figure 6. Static pressure versus nozzle length: IMP PAN experiment and calculations.

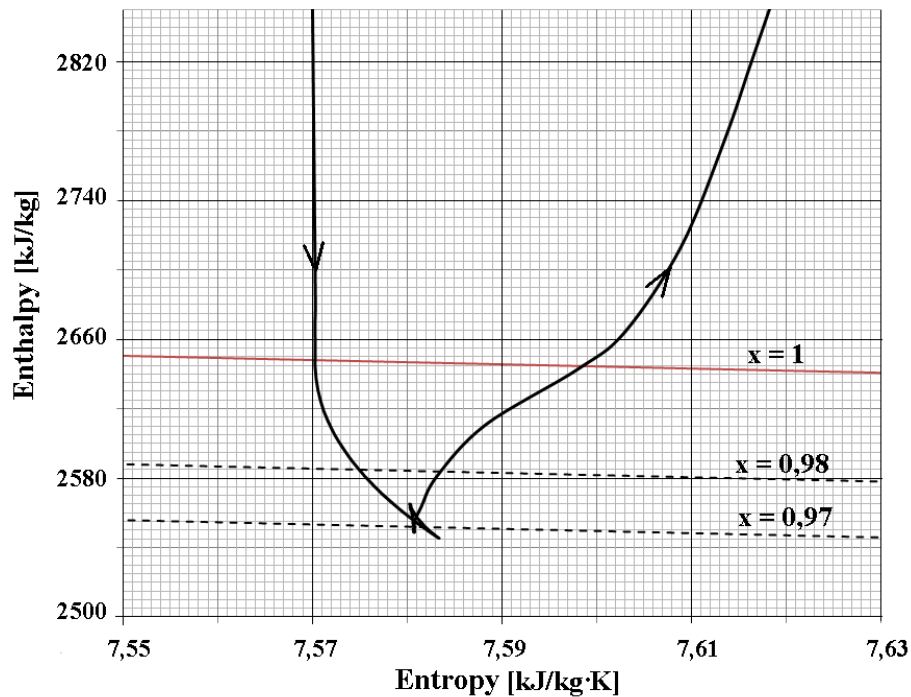


Figure 7. Change of steam entropy during nozzle expansion.

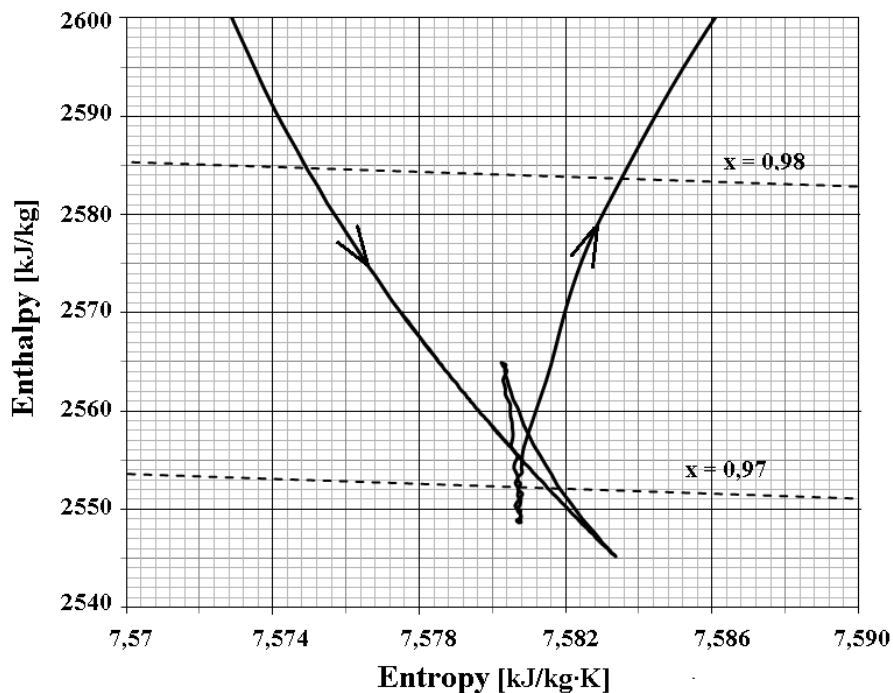


Figure 8. Change of steam entropy during nozzle expansion – a detail.

Figure 9 shows wetness for calculation of CFD simulation for the V-th set of experimental conditions. Results of our analysis (condensation and shock wave) is the same like in Puzyrewski's experiment: *For V-th set of experimental conditions, there were only very slight traces of mist ahead of the shock*

wave, disappearing in the shock. Due to the increase of steam conditions through the wave, there is a complete evaporation of the condensed water drops.

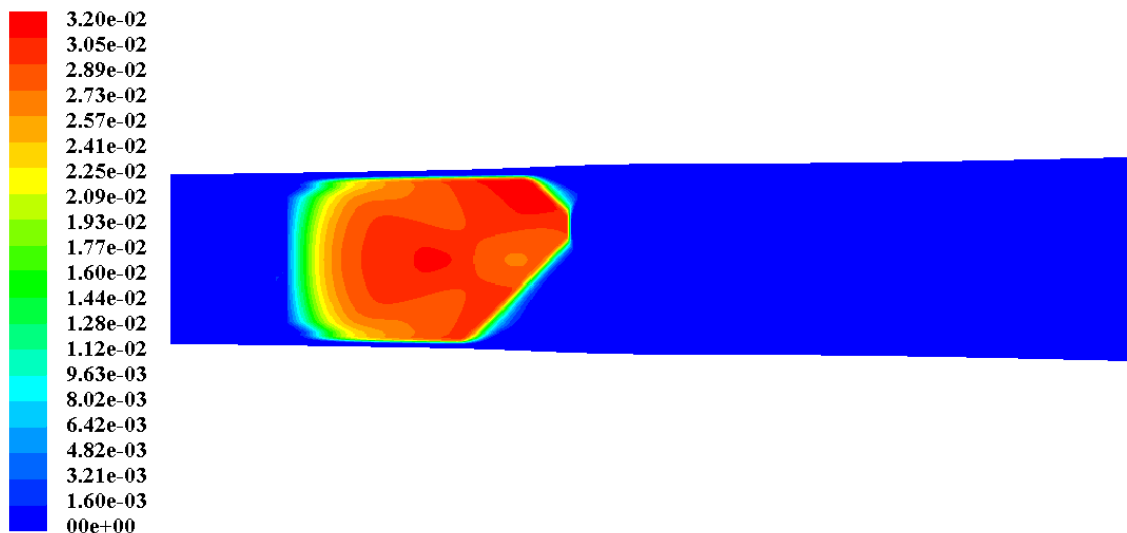


Figure 9. Frog appearing and mist disappearing in the shock for a CFD analysis.

6. Conclusions

Models of nine-equation non-equilibrium have been tested and compared with experimental data. This Wet-Steam model applied to de Laval nozzle gives satisfactory results that agree well with experimental data. Presented data indicates correctness and utilization of employed model for condensing flows in more complex geometries.

Our numerical investigation have shown that for low Mach numbers the feet are of the same size. However, at certain Mach values ($Ma > 1.4$), the shock pattern becomes asymmetric. λ -feet generated on the upper and lower walls of a symmetric planar nozzle become different in size for $Ma > 1.4$. This phenomena is depending on interaction between a normal shock wave and the boundary layer.

7. References

- [1] Puzyrewski R 1969 Theoretical and experimental studies on formation and growth of water drops in LP steam turbines *Transactions of IFFM* **42-44** 289-303
- [2] Bilicki Z, Badur J 2003 A thermodynamically consistent relaxation model for a turbulent, binary mixture undergoing phase transition *Journal of Non-Equilibrium Thermodynamics* **28** 145-172
- [3] Namieśnik K, Doerffer P 2004 Numerical simulation of shock wave patterns in supersonic divergent symmetric nozzles *TASK QUARTERLY* **9** 53-63
- [4] Puzyrewski R, Gardzielwicz A, Bagińska M 1973 Shock wave in condensing steam flow through a Laval nozzle, *Archives of Mechanics* **25**, 3 393-409
- [5] Zakrzewski W 2011 Walidacja modelu pary mokrej przez porównanie z eksperymentem, *Współczesne technologie i konwersja energii*, Wydawca Wydział Mechaniczny
- [6] Dykas S, Majkut M, Smółka K, Stozin M 2013 Reserach on steam condensation flow in nozzle with shock wave *Journal of Power Technologies* vol 93 No 5
- [7] Bourgoing A, Reijasse Ph 2005 Experimental analysis of unsteady separated flows in a supersonic planar nozzle *Shock Waves* **14** (4) 251-258
- [8] Sellam M, Fournier G, Chpoun A, Reijasse Ph 2014 Numerical investigation of overexpanded nozzle flow *Shock Wave* **24** 33-39

- [9] Verma S B, Manisanka C 2014 Origin of flow asymmetry in planar nozzle with separation *Shock Wave* **24** 191-209
- [10] Badur J, Karcz M, Lemański M, Zakrzewski W, Jesionek K 2011 Remarks on steam condensation modeling related to steam turbine of large output *Proc. of microCAD "International Scientific Conference"*, Miscolec
- [11] Karcz M, Zakrzewski W, Lemański M, Badur J 2011 Zagadnienia modelowanie 3D spontanicznej kondensacji w części niskoprężnej turbiny parowej 200MW *Mat. X Konf. Nauk.-Tech. „Elektrownie Ciepłne Eksploatacja-Modernizacje-Remonty"*, Słok k.Bełchatowa 253-262